Am J Transl Res 2025;17(11):8555-8566
www.ajtr.org /ISSN:1943-8141/AJTR0167702

Original Article

Synergistic antitumor efficacy of CIK cells combined with PD-1 inhibitors in nasopharyngeal carcinoma

Jing Chen[1], Tumaer Sailihan[2], Yanhong Chen[2], Suzhen Xv[1], Jiong Qian[1], Xinyi Shen[2], Hangjing Yang[3], Pan Zhang[2]

[1]*Department of Medical Oncology, The First Affiliated Hospital of College of Medicine, Zhejiang University, Hangzhou 310003, Zhejiang, China;* [2]*Laboratory Animal Center of Zhejiang University, Hangzhou 310058, Zhejiang, China;* [3]*Department of Pathology, The First Affiliated Hospital of College of Medicine, Zhejiang University, Hangzhou 310003, Zhejiang, China*

Received July 25, 2025; Accepted October 15, 2025; Epub November 15, 2025; Published November 30, 2025

Abstract: Objectives: To investigate the synergistic anti-tumor effects and underlying mechanisms of combining cytokine-induced killer (CIK) cell therapy with programmed death 1 (PD-1) blockade in the treatment of nasopharyngeal carcinoma (NPC). Methods: CIK cells were generated from peripheral blood mononuclear cells (PBMCs) of healthy donors. The combinatorial effects were assessed *in vitro* by co-culturing CIK cells with HK-1 NPC cells to assess cytotoxicity, apoptosis-related gene expression, cytokine secretion, and activation of the mitogen-activated protein kinase kinase (MEK)/extracellular signal-regulated kinase (ERK) pathway. *In vivo* efficacy was evaluated in a NOD scid gamma (NSG) mouse xenograft model (n=6/group). Results: *In vitro*, PD-1 blockade dose-dependently enhanced CIK cell-mediated cytotoxicity, apoptosis, and secretion of interferon-gamma (IFN-γ), tumor necrosis factor-alpha (TNF-α), and interleukin-2 (IL-2), concomitant with MEK/ERK pathway activation. *In vivo*, combination therapy significantly inhibited tumor growth compared with either monotherapy. This was associated with increased infiltration of cluster of differentiation (CD)3$^+$, CD4$^+$, CD8$^+$, and CD56$^+$ immune cells, enhanced tumor apoptosis (TUNEL+), reduced proliferation (Ki67), and alleviated oxidative stress within the tumor microenvironment. Conclusions: Combined CIK cell therapy and PD-1 blockade demonstrated significant synergistic anti-tumor activity against NPC by enhancing cytotoxicity, activating key signaling pathways, and remodeling the tumor immune microenvironment. This strategy represents a promising therapeutic approach for NPC.

Keywords: CIK, PD-1, combination, nasopharyngeal carcinoma, signal pathway

Introduction

Epithelial cells within the nasopharynx give rise to nasopharyngeal carcinoma (NPC), with a high incidence in Southeast Asia and Southern China [1, 2]. Despite advancements in radiotherapy and chemotherapy, the prognosis for advanced NPC remains poor due to frequent local recurrences and distant metastases [3]. This inference underscores the urgent need for novel combination therapies. Combining cytokine-induced killer (CIK) cells with programmed death receptor protein 1 (PD-1) inhibitors, as an adjuvant approach, has shown promise in augmenting anti-tumor immune responses [4, 5]. However, the therapeutic potential of this combination has not been thoroughly investigated in NPC.

Immunotherapy has emerged as an option for improving NPC treatment outcomes [6, 7]. Recent research has advanced our understanding of immune evasion mechanisms in NPC, implicating several critical factors; these encompass the equilibrium between effector and regulatory T cells, physical barriers within the tumor microenvironment, and immunosuppressive signaling pathways. For instance, Geels et al. elucidated the dual function of CD8$^+$ T cells in anti-PD-1 therapy and proposed that concurrent blockade of the inducible T-cell co-stimulator ligand (ICOSL) could counteract immunosuppressive feedback, thereby enhancing therapeutic efficacy [8]. Sargsian et al. reported that silver nanoparticles could induce immunogenic cell death, transforming immunologically "cold" tumors into "hot" ones, thereby enhanc-

https://doi.org/10.62347/RTPJ9684

ing immunotherapy efficacy [9]. Similarly, He Zhuoying et al., identified the restrictive role of the extracellular matrix in T-cell infiltration and suggested that inhibition of Discoidin Domain Receptor 1 (DDR1) may further potentiate immune checkpoint blockade [10]. Collectively, these studies underscore a growing trend toward combinational immunotherapy strategies. However, further investigation is required to validate their long-term efficacy, safety, and individualized ause.

CIK cells represent a heterogeneous subset of T lymphocytes with dual characteristics of natural killer (NK) cells and T cells, offering unique anti-tumor capabilities [11, 12]. They recognize and eliminate various solid tumor cells through tumor-associated antigens or non-specific pathways independent of the major histocompatibility complex (MHC), rendering them exceptionally adaptable for clinical applications [13, 14]. CIK cells have demonstrated robust anti-tumor activity in several malignancies, including lung, liver, and gastric cancers [15]. PD-1 is a critical immune checkpoint molecule. Upon binding to its binding partner ligand, PD-L1, it suppresses T-lymphocyte activation, thereby enabling tumor cells to evade immune surveillance [16, 17]. PD-1 inhibitors (such as nivolumab and pembrolizumab) disrupt this interaction, restoring T-cell effector function and showing remarkable efficacy across various malignancies [18, 19]. These immune checkpoint inhibitors have shown remarkable success in treating melanoma, non-small cell lung cancer, and others [20, 21]. With advancing insight into immunotherapy, combination strategies have emerged as a promising approach to enhance therapeutic efficacy. Combining CIK cells with PD-1 inhibitors yields synergistic effects by directly targeting tumor cells while simultaneously alleviating immune suppression, thereby augmenting both T-cell and CIK cell activity [16, 22]. This combinational approach has shown promise for treating refractory cancers, encompassing renal cell carcinoma and triple-negative breast cancer [23].

Given that the potential of combining CIK cells with PD-1 inhibitors in NPC remains underexplored, this study aimed to investigate the efficacy and safety of this combination using *in vitro* and *in vivo* models. Moreover, this investigation sought to uncover the underlying mechanisms by which this therapeutic strategy enhances anti-tumor immunity. These findings may contribute to developing new combinational strategies for NPC treatment.

Materials and methods

Ethical statement

All animal experiments were performed in accordance with the guidelines approved by the Ethics Committee of The First Affiliated Hospital of College of Medicine, Zhejiang University. The collection and use of human samples were approved by the Ethics Committee of The First Affiliated Hospital of College of Medicine, Zhejiang University.

CIK cell preparation

Human peripheral blood mononuclear cells (PBMCs) were procured from the heparinized blood of five healthy donors by Ficoll density gradient centrifugation. Informed consent was obtained from all participants. The PBMCs were resuspended at 1×10^6 cells/mL in Roswell Park Memorial Institute (RPMI, Gibco, USA) 1640 medium comprising 10% fetal bovine serum (FBS, Gibco, USA). To promote CIK cell differentiation, the cells were cultured with monoclonal anti-CD3 antibodies (GenScript, China), recombinant human interleukin-2 (IL-2, CoSinCayon, China), IL-1α (CoSinCayon, China), and interferon-γ (IFN-γ, CoSinCayon, China). The medium was replaced every 5 days, with cultures continuing for 21 days. On day 21, a portion of these cells was harvested for flow cytometric analysis to examine the expression of surface markers on the primary effector cells using anti-CD3-Fluorescein Isothiocyanate (FITC, Thermo Fisher Scientific Inc., USA) and anti-CD56-Phycoerythrin (PE) antibodies (Cytognos S.L, Spain), to monitor changes in the CIK cell phenotype.

In vitro tumor cell killing assay

CIK cells, induced and expanded as previously described, were co-cultured with revived HK-1 cells at specific effector-to-target (E:T) proportions (10:1, 20:1, and 40:1) in 6-well plates (Thermo Fisher Scientific Inc., USA), with three replicates per ratio. HK-1 cells were prepared at a concentration of 5×10^4/mL and seeded into the lower chamber of the 6-well plates comprising 0.4 μm pore-sized Transwell inserts, while

Table 1. Primers for qPCR

Primer	Sequence (5'-3')
Caspase-3-F	ATGGAAGCGAATCAATGGA
Caspase-3-R	TGTACCAGACCGAGATGTC
Bcl-2-F	TCCGATCAGGAAGGCTAGAGTT
Bcl-2-R	TCGGTCTCCTAAAAGCAGGC
Bax-F	CCGCCGTGGACACAGAC
Bax-R	CAGAAAACATGTCAGCTGCCA
GAPDH-F	GAAGGTGAAGGTCGGAGTCA
GAPDH-R	GAAGATGGTGATGGGATTTC

CIK cells were seeded in the upper chamber. The control cohort consisted of HK-1 cells cultured alone, with three replicates. In experimental cohorts, PD-1 monoclonal antibody (GenScript, China) was introduced at doses of 1 μg/mL and 10 μg/mL, whereas PBS of equivalent volume served as the control.

After 48 hours of incubation at 37°C in 5% CO_2, apoptosis-related gene expression in tumor cells was assessed by quantitative polymerase chain reaction (qPCR). Total RNA was isolated from cells in each experimental group, followed by reverse transcription to generate complementary DNA (cDNA). SYBR Green real-time qPCR kits (Vazyme, China) were used to measure mRNA levels of *caspase-3*, B-cell lymphoma 2 (*Bcl-2*), and Bcl-2-associated X protein (*Bax*). Primer sequences are shown in **Table 1**. GAPDH served as an internal control, and the qPCR reactions were conducted according to the supplier's instructions. In parallel, cytokine production was assessed using enzyme-linked immunosorbent assay (ELISA). Supernatants from the co-culture system were harvested, and the concentrations of IFN-γ, TNF-α, IL-2, and IL-6 were quantified utilizing ELISA kits (ml106726 etc., mlBio, China).

Mitogen-activated protein kinase/extracellular signal-regulated kinase (MEK/ERK) pathway analysis in CIK cells by western blot

CIK cells from the high-concentration co-culture system were harvested, and total protein was extracted using RIPA lysis buffer (Beyotime, P0013C) containing protease and phosphatase inhibitors. Protein concentration was determined using a BCA assay kit (Beyotime, P0009). For each sample, 20 μg of protein was separated by 10% SDS-PAGE and transferred to PVDF membranes (Merck Millipore, USA). The membranes were blocked with 5% non-fat milk for 1 hour at room temperature and then incubated overnight at 4°C with the following primary antibodies: anti-ERK (1:1000, NewEast Biosciences, China), anti-p-ERK (1:1000, NewEast Biosciences, China), anti-MEK (1:1000, NewEast Biosciences, China), anti-p-MEK (NewEast Biosciences, China), and anti-GAPDH (1:5000, NewEast Biosciences, China) as a loading control. Subsequently, the membranes were incubated with HRP-conjugated secondary antibodies (1:5000, Beyotime, China) for 1 hour at room temperature. Protein bands were visualized using an ECL detection system (Beyotime, China). Band densities were quantified using ImageJ software, and the expression levels of target proteins were normalized to GAPDH.

In vivo tumor xenograft experiment

Animal experiments were conducted at the Zhejiang University Medical Animal Center. Six-week-old male NSG mice (Charles River, China) were randomly assigned to four cohorts (n=6 per cohort): the negative control cohort, CIK cell cohort, anti-PD-1 monoclonal antibody cohort, and CIK + anti-PD-1 monoclonal antibody cohort. To establish the xenograft tumor model, HK-1 cells (2×10^6) were inoculated subcutaneously near the right axillary region of each specimen. Treatment was initiated once the tumor volume reached 500 mm^3. The CIK cohort received intravenous injections of 1×10^8 CIK cells, the anti-PD-1 cohort received intravenous injections of anti-PD-1 monoclonal antibody (10 mg/kg), and the CIK + anti-PD-1 cohort received both treatments. The negative control cohort received an equivalent volume of PBS solution. Treatments were administered weekly for three weeks. Tumor size was measured with calipers every two days, and tumor volume was calculated using the formula: $V = 0.5 \times a \times b^2$, where "a" is the length and "b" is the width of the tumor. Tumor fold change growth (FCTG) was calculated as: FCTG = (Ve - V0)/V0, where V0 is the pre-treatment tumor volume, and Ve is the post-treatment tumor volume. An FCTG < 2 indicated effective tumor growth inhibition. At the end of the experiment, the mice were euthanized by CO_2 asphyxiation followed by cervical dislocation, in accordance with the AVMA Guidelines for the Euthanasia of Animals. The tumors, spleens, and serum samples were procured for subsequent examination. The study

was approved by the institutional ethics committee (approval number: IIT20240567B).

CIK cell infiltration

Immunohistochemical analysis was conducted on tumor and spleen tissues to assess CIK cell infiltration using markers including $CD3^+$, $CD4^+$, $CD8^+$, and $CD56^+$. For each mouse, sections of both tumor and spleen tissues were subjected to immunohistochemical staining with all four antibodies (C7930, Merck Sigma-Aldrich, USA).

Apoptosis detection and enzyme activity assay in tumor tissue

Terminal deoxynucleotidyl transferase dUTP nick end labeling (TUNEL) and Ki67 immunofluorescence staining were performed to assess apoptosis in tumor tissues. Supernatants from homogenized tumor tissues were collected, and enzyme activity assays were performed to measure the levels of superoxide dismutase (SOD) (ab65354, Abcam plc., UK), malondialdehyde (MDA) (ab238537, Abcam plc., UK), glutathione peroxidase (GPX) (ml107243, mlBio, China), and catalase (CAT) (ab83464, Abcam plc., UK) using commercially available kits per the supplier's protocols.

Statistical analysis

Data were presented as mean ± standard deviation (mean ± SEM). Comparisons between two independent cohorts were executed utilizing Student's t-test, while one-way analysis of variance (ANOVA) with Tukey's post hoc test was employed for multiple cohort comparisons. Trends in continuous variables, encompassing tumor volume and cytokine levels, were analyzed using repeated-measures ANOVA. A *P*-value < 0.05 was considered significant. All statistical analyses were executed utilizing GraphPad Prism 6.0 software.

Results

CIK cell preparation

Flow cytometric analysis demonstrated a notable elevation in the proportion of $CD3^+$, $CD56^+$ cells in CIK cell cultures after 21 days of induction, compared to pre-induction levels ($P < 0.01$), indicating successful CIK cell induction (**Figure 1A**).

In vitro tumor cell killing assay

In the CIK cell-treated cohort, mRNA levels of caspase-3 and Bax in HK-1 cells were upregulated, while Bcl-2 expression was reduced compared to the model cohort. The addition of PD-1 antibodies further enhanced the levels of caspase-3 and Bax and suppressed Bcl-2 expression in a dose-dependent manner (**Figure 1B**). Moreover, the secretion of IFN-γ, TNF-α, and IL-2 in the supernatant from the CIK-treated cohort was higher than that in the control cohort. Upon the addition of PD-1 antibodies, the secretion of these cytokines increased further (**Figure 1C**). These findings indicate that PD-1 antibodies augmented the capacity of CIK cells to trigger apoptosis in HK-1 cells.

MEK/ERK pathway in CIK cells

Western blot analysis revealed that the co-treatment of CIK cells with PD-1 antibodies significantly increased the levels of phosphorylated ERK (p-ERK) and phosphorylated MEK (p-MEK) compared to CIK cell treatment alone. The total ERK and MEK protein expression remained unaltered (**Figure 1D**). These results imply that PD-1 antibodies may enhance the anti-tumor effects of CIK cells by activating the MEK/ERK signaling pathway.

In vivo tumor growth

Both CIK cell treatment and combination therapy significantly suppressed tumor progression in mice. The combination of CIK cells with PD-1 antibodies further slowed tumor growth, with volumes considerably smaller than those in the single-agent or control cohorts, indicating a synergistic anti-tumor effect. The FCTG value was lowest in the combination therapy cohort, confirming its superior ability to inhibit tumor growth (**Figure 2A**, **2B**). To assess systemic toxicity, the body weights of the mice were monitored throughout the experiment. No significant weight loss was observed in any of the treatment groups compared to the control group. Furthermore, at the end of the study, the weights of major organs, including the spleen, showed no significant differences across the cohorts (**Figure 2C**). These findings suggest that the CIK cell therapy and anti-PD-1 antibody treatment, both individually and in combination, were well-tolerated by the animals.

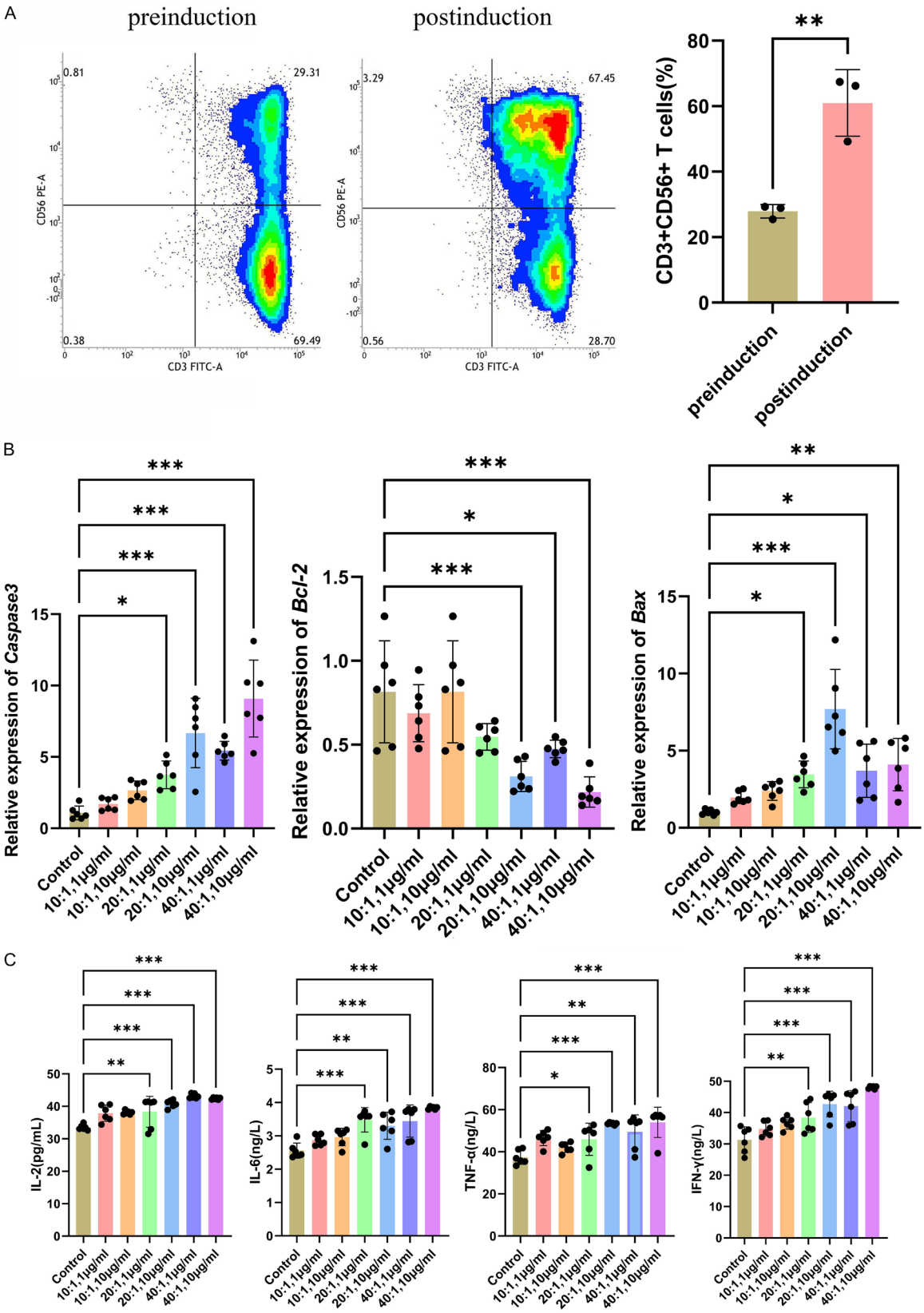
A
preinduction
postinduction
0.81
29.31
0.38
69.49
3.29
67.45
0.56
28.70
CD56 PE-A
CD3 FITC-A
CD3+CD56+ T cells(%)
preinduction
postinduction
B
Relative expression of Caspase3
Relative expression of Bcl-2
Relative expression of Bax
Control
10:1,1μg/ml
10:1,10μg/ml
20:1,1μg/ml
20:1,10μg/ml
40:1,1μg/ml
40:1,10μg/ml
C
IL-2(pg/mL)
IL-6(ng/L)
TNF-α(ng/L)
IFN-γ(ng/L)

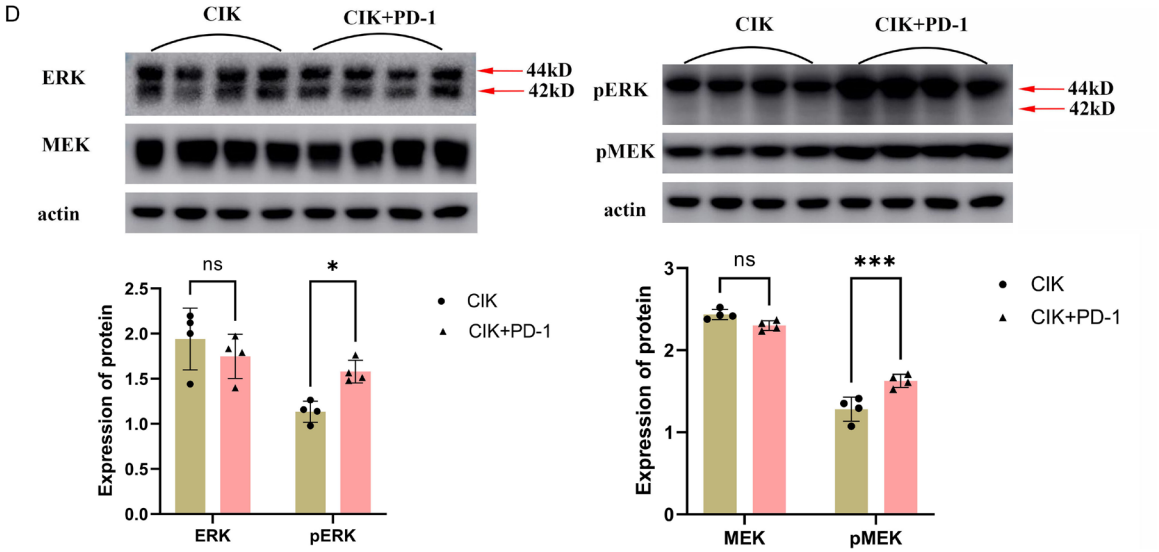

Figure 1. Phenotypic identification and functional analysis of CIK cells. A. Surface marker assessment by flow cytometry illustrating CD3 and CD56 expression patterns on CIK cells. B. Real-time quantitative PCR showing the mRNA levels of apoptosis-related genes, encompassing *caspase3*, *BAX*, and *Bcl-2*. C. ELISA analysis indicating cytokine secretion levels of IL-2, IL-6, TNF-α, and IFN-γ. D. Western blot (WB) analysis of proteins involved in key signaling pathways, including ERK and MEK in CIK cells. Data are denoted as mean ± standard error of the mean (SEM). *P < 0.05, **P < 0.01, ***P < 0.001, ns, not significant (compared to the control cohort).

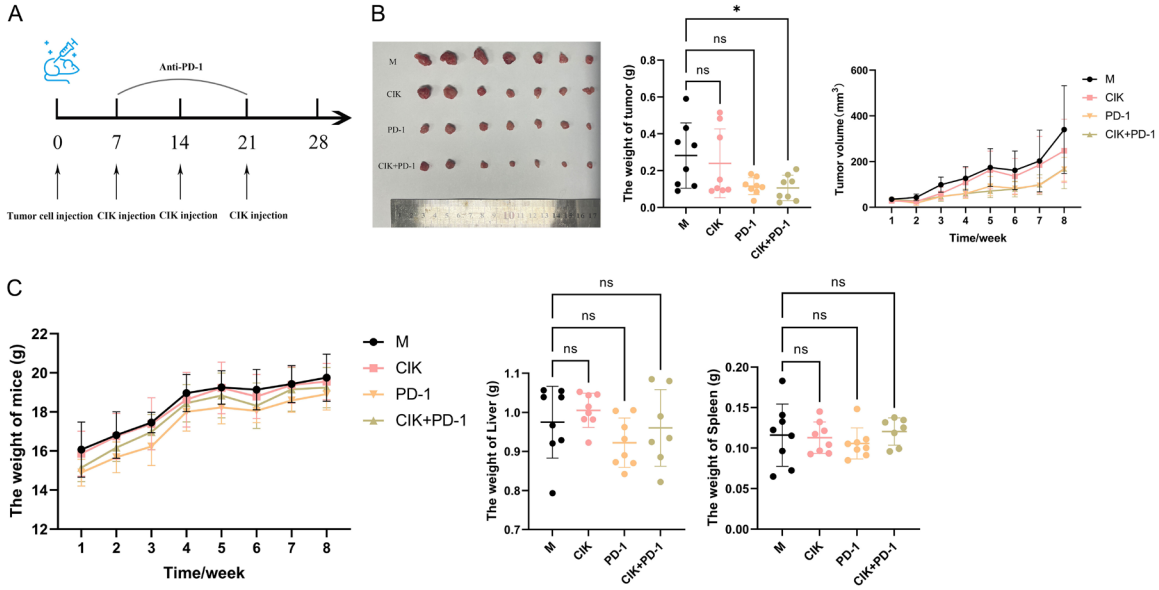

Figure 2. Combined PD-1 antibody and CIK cell therapy in a mouse xenograft tumor model. A. Schematic representation of the treatment protocol with PD-1 antibodies and CIK cells, detailing three sequential injections. B. Images and tumor growth data for mice treated with PBS (control), CIK cells, PD-1 antibodies or combination therapy (CIK+PD-1). Each cohort included six mice (n=6). C. Changes in mice weight and organs. *P < 0.05, **P < 0.01, ***P < 0.001, ns, not significant (vs. the model cohort).

Enzyme activity assay results

Immunohistochemical analysis showed that CIK cell treatment increased the infiltration of $CD3^+$, $CD4^+$, $CD8^+$, and $CD56^+$ cells in both tumor and spleen tissues compared to the control cohort. The addition of PD-1 antibodies further enhanced immune cell infiltration (**Figure 3**), suggesting that the combination therapy promotes a more substantial infiltration and

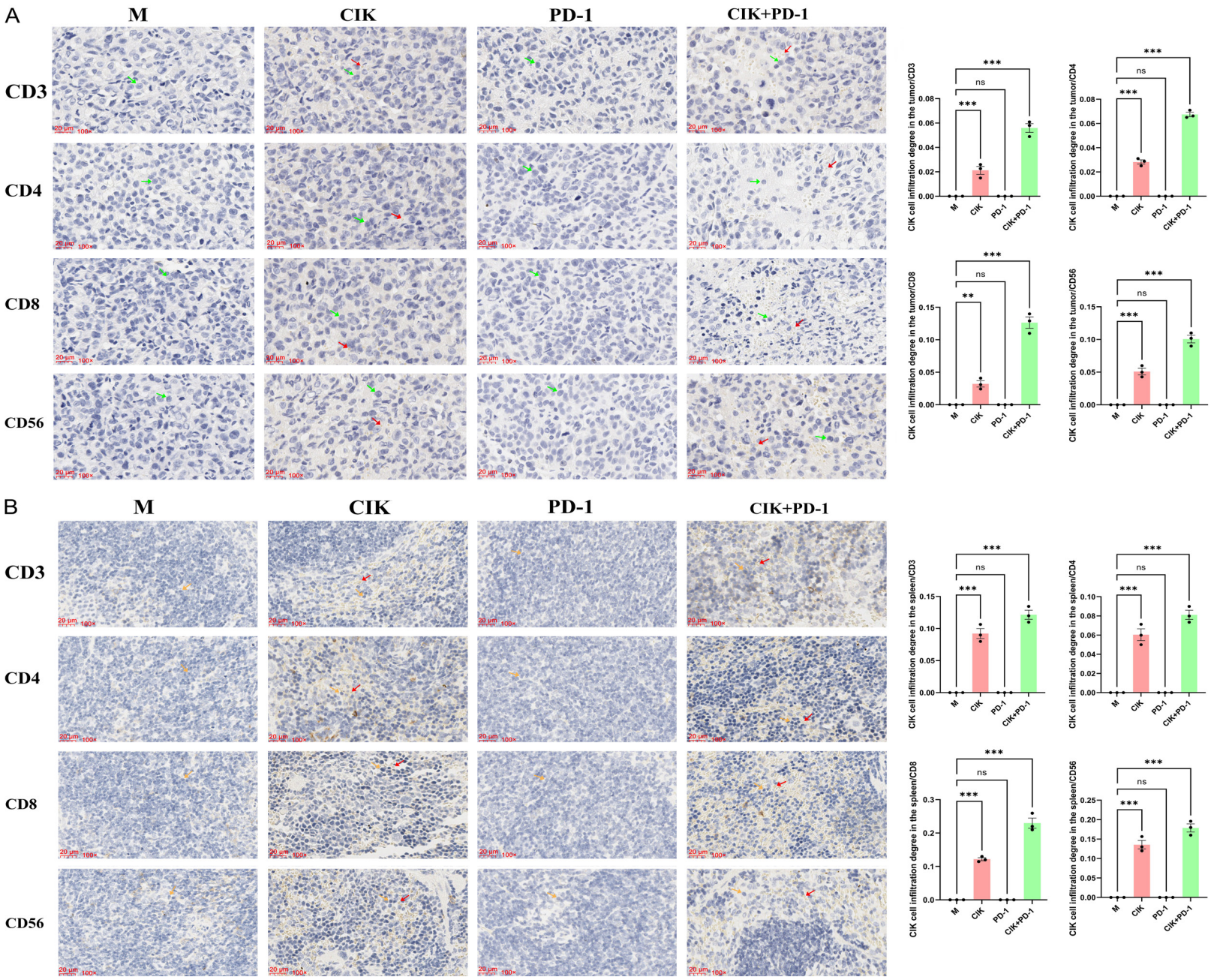
A
M
CIK
PD-1
CIK+PD-1
CD3
CD4
CD8
CD56
CIK cell infiltration degree in the tumor/CD3
CIK cell infiltration degree in the tumor/CD4
CIK cell infiltration degree in the tumor/CD8
CIK cell infiltration degree in the tumor/CD56
B
CIK cell infiltration degree in the spleen/CD3
CIK cell infiltration degree in the spleen/CD4
CIK cell infiltration degree in the spleen/CD8
CIK cell infiltration degree in the spleen/CD56
***
**
ns

Figure 3. Immunohistochemical analysis shows CD3, CD4, CD8, and CD56 expression in tumor (A) and spleen (B) tissues from treated mice. Green arrows indicate nasopharyngeal carcinoma cells and red arrows indicate CIK cells. Orange arrows indicate spleen cells and red arrows indicate CIK cells. *P < 0.05, **P < 0.01, ***P < 0.001, ns, not significant.

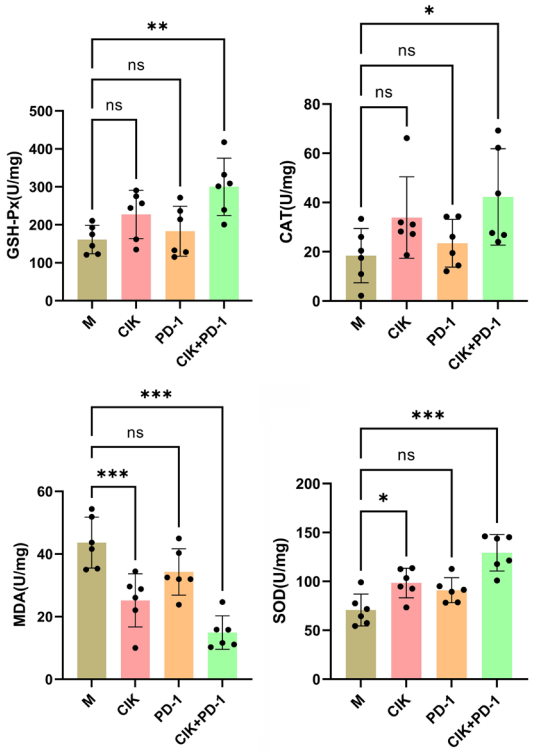

Figure 4. Enzyme activity assays quantifying antioxidant enzymes GSH, CAT, SOD, and the lipid peroxidation product MDA in mouse tumor tissues. *P < 0.05, **P < 0.01, ***P < 0.001, ns, not significant (vs. the control cohort).

activation of effector immune cells. Furthermore, combination therapy notably elevated the levels of SOD, GPX, and CAT in tumor tissues, while reducing MDA levels ($P < 0.05$) (**Figure 4**), suggesting a reduction in oxidative stress in the tumor microenvironment.

Tumor tissue apoptosis detection

The TUNEL assay demonstrated that both CIK cells and PD-1 antibodies induced apoptosis in tumor cells compared to the control cohort, with the combination therapy cohort exhibiting the highest number of apoptotic cells (**Figure 5A**). However, Ki67 immunofluorescence staining further revealed the lowest number of Ki67-positive cells in the combination therapy cohort, indicating the most significant inhibition of tumor cell proliferation (**Figure 5B**).

Discussion

Nasopharyngeal carcinoma is a malignancy originating from the nasopharyngeal epithelium, characterized by a unique geographical distribution and a strong association with Epstein-Barr virus (EBV) infection [24, 25]. This study investigated the therapeutic potential and underlying mechanisms of combining CIK cells with PD-1 inhibitors in NPC treatment. The results revealed synergistic effects, exhibiting enhanced anti-tumor efficacy in both *in vitro* and *in vivo* models.

The CIK cells were successfully induced and expanded, and their phenotype was consistent with previous studies [26]. *In vitro*, CIK cells induced apoptosis in HK-1 cells by upregulating pro-apoptotic genes, downregulating anti-apoptotic genes, and secreting cytokines such as IFN-γ, TNF-α, and IL-2. The addition of PD-1 antibodies further enhanced these effects, suggesting that PD-1 antibodies further potentiated the cytotoxicity of CIK cells by relieving immune suppression. Western blot analysis further indicated that PD-1 antibodies likely exert these effects by stimulating the MEK/ERK signaling cascade in CIK cells. The MEK/ERK pathway is essential for regulating T-cell activation, proliferation, and effector functions [27], supporting our findings that PD-1 inhibition enhances CIK cell-mediated cytotoxicity, promotes a pro-inflammatory cytokine profile, and activates the MEK/ERK pathway.

Research into the PD-1/PD-L1 axis continues to unveil its crucial role in tumor immune evasion, involving complex molecular interactions. Studies by Yu et al. on Mind bomb 2 (MIB2) and Liu et al. on the Tryptophan-Receptor Complex-Kynurenine-Aryl Hydrocarbon Receptor-Programmed Cell Death Protein 1 (TRC-Kyn-AhR-PD-1) pathway provide fresh insights into modulating PD-1/PD-L1 activity in the tumor immune microenvironment [28, 29]. Li et al.'s Mendelian randomization analysis linking PD-1/PD-L1 to circulating biomarkers opens a promising avenue for understanding the genetic regulation of immune checkpoints [30]. Furthermore, Rohit et al.'s molecular dynamics

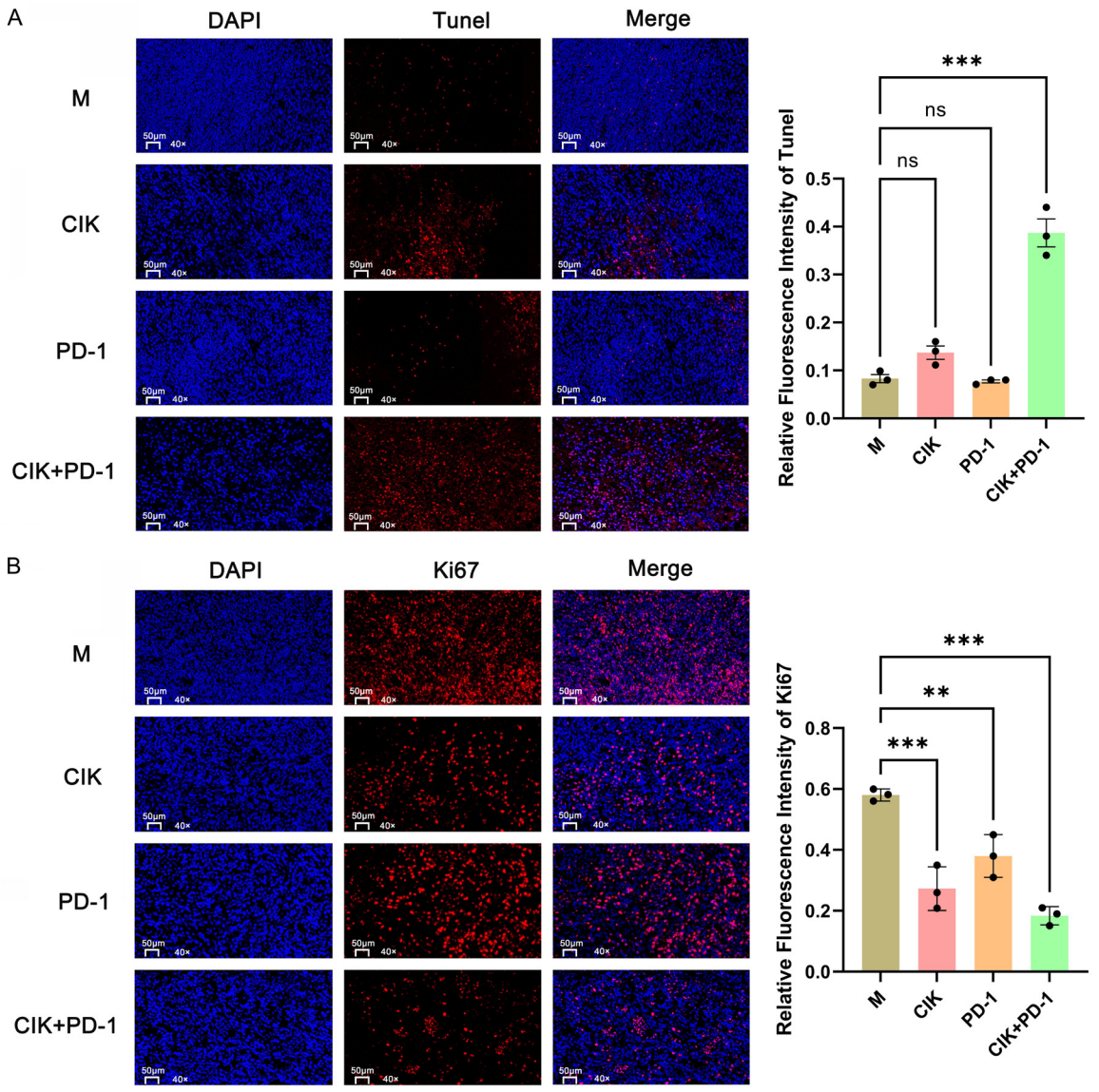

Figure 5. Analysis of proliferation and apoptosis in tumor tissues. A. TUNEL staining to detect apoptosis in tumor tissues. TUNEL-positive cells (red) indicate apoptotic cells; the higher the number of positive cells, the higher the level of apoptosis. B. Ki67 immunohistochemical staining to evaluate the proliferative capacity of tumor tissues. Ki67-positive cells (red) represent proliferating cells. The higher the number of positive cells, the stronger the proliferative capacity. *P < 0.05, **P < 0.01, ***P < 0.001, ns, not significant.

simulation and Pal et al.'s development of a novel PD-L1 imaging technique offer valuable perspectives on PD-1 and PD-L1 expression [31, 32]. The development of small molecules like glutamine (threonine-transferase) [Gln(TrT)] by Li et al., which simultaneously inhibits the T-cell immunoreceptor with Ig and ITIM domains (TIGIT)/Poliovirus Receptor (PVR) and PD-1/PD-L1 pathways, along with Yoon et al.'s use of a mRNA-encoded monoclonal antibody against CD3 (MA-aCD3) for *in situ* tumor-infiltrating lymphocyte (TIL) therapy, underscore the potential of dual or multi-target immune checkpoint inhibition strategies [33, 34]. These studies highlight a shift towards more complex, multi-target approaches for cancer immunotherapy.

In our study, both CIK cell therapy and PD-1 antibody treatment significantly suppressed tumor growth in the NSG mouse xenograft model, with the combination therapy demonstrating even greater tumor inhibition. Pathologic analysis revealed that the combination therapy en-

hanced tumor cell apoptosis, increased immune cell infiltration in the tumor and spleen, and reduced tumor volume compared to single-agent therapies, confirming the synergistic effects. These findings align with previous research indicating that combination immunotherapy can produce synergistic anti-tumor effects by enhancing antigen presentation, reversing immunosuppressive microenvironment, and promoting effector cell infiltration [35, 36].

Moreover, our study observed that the combination therapy improved oxidative stress levels in tumor tissues, possibly contributing to its enhanced efficacy, as reduced oxidative stress can benefit immune cell function. Recent advances in improving CIK cell anti-tumor efficacy have provided valuable insights and experimental evidence for developing innovative cancer immunotherapy strategies, including targeting molecular pathways, microRNA regulation, and innovative pharmacologic formulations. Patel et al. showed that the transcription factor GATA binding protein 4 (GATA4) promotes tumor suppression by recruiting cytotoxic CD8 T cells and enhances the effect of anti-PD-1 therapy, highlighting the potential of these targets in immunotherapy [37]. Wang et al. identified specific microRNA clusters regulating cell proliferation and tumor cytotoxic, providing a new perspective for optimizing CIK cell therapy [38]. Furthermore, novel pharmacological combinations, such as those explored by Chen et al., have demonstrated the potential of combining CIK therapy with immune checkpoint inhibitors to enhance therapeutic outcomes [39]. This suggests that the combination of CIK cells and PD-1 inhibitors not only boosts the direct anti-tumor immune response but also remodels the tumor microenvironment by increasing immune cell infiltration and alleviating oxidative stress, thereby creating a more favorable landscape for sustained tumor destruction.

Despite the promising findings, this study has several limitations that should be acknowledged. First, our *in vitro* and *in vivo* experiments were conducted using a single NPC cell line (HK-1), which may not fully capture the heterogeneity of the disease. Second, the use of severely immunodeficient NSG mice, while essential for xenografting human cells, limits our ability to assess the therapy's interaction with a fully functional host immune system, including the role of host antigen-presenting cells. However, these limitations provide a basis for future investigation. Future studies should aim to validate these synergistic effects across a broader panel of NPC cell lines and, more importantly, in patient-derived xenograft (PDX) models. Furthermore, employing humanized mouse models could provide deeper insight into the complex interplay between infused CIK cells, the tumor, and the host's immune components under PD-1 blockade. Overall, the promising preclinical evidence from this study provides a strong rationale for advancing this combination immunotherapy strategy into clinical trials, particularly for patients with advanced or recurrent NPC, a population with urgent unmet medical needs.

Conclusion

The effectiveness and underlying mechanisms of combining CIK cells with PD-1 inhibitors in treating NPC were evaluated through *in vitro* and *in vivo* experiments. The combination therapy demonstrated enhanced anti-tumor effects, likely by inducing tumor cell apoptosis, activating the MEK/ERK signaling pathway in CIK cells, promoting immune cell infiltration, and improving the tumor microenvironment. Although further clinical investigations are needed to assess its sustained efficacy and safety, these results suggest that this combination therapy holds promise as an effective immunotherapeutic strategy for NPC.

Acknowledgements

This work was supported by the Natural Sciences Fund of Zhejiang Province (LGF22H160019).

Disclosure of conflict of interest

None.

Address correspondence to: Jing Chen, Department of Medical Oncology, The First Affiliated Hospital of College of Medicine, Zhejiang University, No. 79, Qingchun Road, Hangzhou 310003, Zhejiang, China. Tel: +86-0571-87236668; E-mail: chenjingmed@sina.cn

References

[1] Dee EC, Eala MA, Feliciano EJG, Jacomina LE, Chua MLK, Mejia MB and Lee NY. Nasopharynx cancer in Southeast Asia: an analysis of

2022 incidence and mortality. International Journal of Radiation Oncology Biology Physics 2024; 120: e746-e747.
[2] Bai R, Sun J, Xu Y, Sun Z and Zhao X. Incidence and mortality trends of nasopharynx cancer from 1990 to 2019 in China: an age-period-cohort analysis. BMC Public Health 2022; 22: 1351.
[3] Chen YP, Chen Y, Zhang WN, Liang SB, Zong JF, Chen L, Mao YP, Tang LL, Li WF, Liu X, Guo Y, Lin AH, Liu MZ, Sun Y and Ma J. Potential surrogate endpoints for overall survival in locoregionally advanced nasopharyngeal carcinoma: an analysis of a phase III randomized trial. Sci Rep 2015; 5: 12502.
[4] Li Y, Sharma A, Wu X, Weiher H, Skowasch D, Essler M and Schmidt-Wolf IGH. A combination of cytokine-induced killer cells with PD-1 blockade and ALK inhibitor showed substantial intrinsic variability across non-small cell lung cancer cell lines. Front Oncol 2022; 12: 713476.
[5] Dai C, Lin F, Geng R, Ge X, Tang W, Chang J, Wu Z, Liu X, Lin Y, Zhang Z and Li J. Implication of combined PD-L1/PD-1 blockade with cytokine-induced killer cells as a synergistic immunotherapy for gastrointestinal cancer. Oncotarget 2016; 7: 10332-10344.
[6] Kwong DLW. Locoregionally advanced nasopharyngeal carcinoma: integrating immunotherapy into definitive treatment. Lancet Oncol 2024; 25: 1511-1513.
[7] Liu K, Zhu Y, Li S and Zhu H. Chemoradiotherapy plus immunotherapy for locoregionally advanced nasopharyngeal carcinoma: a cost-effectiveness analysis. Head Neck 2025; 47: 485-494.
[8] Geels SN, Moshensky A, Sousa RS, Murat C, Bustos MA, Walker BL, Singh R, Harbour SN, Gutierrez G, Hwang M, Mempel TR, Weaver CT, Nie Q, Hoon DSB, Ganesan AK, Othy S and Marangoni F. Interruption of the intratumor $CD8^+$ T cell: treg crosstalk improves the efficacy of PD-1 immunotherapy. Cancer Cell 2024; 42: 1051-1066, e7.
[9] Sargsian A, Koutsoumpou X, Girmatsion H, Egil Ç, Buttiens K, Luci CR, Soenen SJ and Manshian BB. Silver nanoparticle induced immunogenic cell death can improve immunotherapy. J Nanobiotechnology 2024; 22: 691.
[10] He Z, Zhou X, Xiao Y and Gao Y. In vitro screening methods of novel immune checkpoint inhibitors related to T cell infiltration and anti-PD-1 resistance. Methods Cell Biol 2024; 190: 11-24.
[11] Chen D, Sha H, Hu T, Dong S, Zhang J, Liu S, Cao H, Ma R, Wu Y, Jing C, Wang Z, Wu J and Feng J. Cytokine-induced killer cells as a feasible adoptive immunotherapy for the treatment of lung cancer. Cell Death Dis 2018; 9: 366.
[12] Zhang Q, Liu XY, Zhang T, Zhang XF, Zhao L, Long F, Liu ZK and Wang EH. The dual-functional capability of cytokine-induced killer cells and application in tumor immunology. Hum Immunol 2015; 76: 385-391.
[13] Wei F, Rong XX, Xie RY, Jia LT, Wang HY, Qin YJ, Chen L, Shen HF, Lin XL, Yang J, Yang S, Hao WC, Chen Y, Xiao SJ, Zhou HR, Lin TY, Chen YS, Sun Y, Yao KT and Xiao D. Cytokine-induced killer cells efficiently kill stem-like cancer cells of nasopharyngeal carcinoma via the NKG2D-ligands recognition. Oncotarget 2015; 6: 35023-35039.
[14] Cappuzzello E, Sommaggio R, Zanovello P and Rosato A. Cytokines for the induction of antitumor effectors: the paradigm of cytokine-induced killer (CIK) cells. Cytokine Growth Factor Rev 2017; 36: 99-105.
[15] Guo Y and Han W. Cytokine-induced killer (CIK) cells: from basic research to clinical translation. Chin J Cancer 2015; 34: 99-107.
[16] Sharpe AH and Pauken KE. The diverse functions of the PD1 inhibitory pathway. Nat Rev Immunol 2018; 18: 153-167.
[17] Rosenzweig N, Dvir-Szternfeld R, Tsitsou-Kampeli A, Keren-Shaul H, Ben-Yehuda H, Weill-Raynal P, Cahalon L, Kertser A, Baruch K, Amit I, Weiner A and Schwartz M. PD-1/PD-L1 checkpoint blockade harnesses monocyte-derived macrophages to combat cognitive impairment in a tauopathy mouse model. Nat Commun 2019; 10: 465.
[18] Wu J, Hong D, Zhang X, Lu X and Miao J. PD-1 inhibitors increase the incidence and risk of pneumonitis in cancer patients in a dose-independent manner: a meta-analysis. Sci Rep 2017; 7: 44173.
[19] Tan S, Zhang CW and Gao GF. Seeing is believing: anti-PD-1/PD-L1 monoclonal antibodies in action for checkpoint blockade tumor immunotherapy. Signal Transduct Target Ther 2016; 1: 16029.
[20] Mahoney KM, Freeman GJ and McDermott DF. The next immune-checkpoint inhibitors: PD-1/PD-L1 blockade in melanoma. Clin Ther 2015; 37: 764-782.
[21] Tang J, Yu JX, Hubbard-Lucey VM, Neftelinov ST, Hodge JP and Lin Y. Trial watch: the clinical trial landscape for PD1/PDL1 immune checkpoint inhibitors. Nat Rev Drug Discov 2018; 17: 854-855.
[22] Liu S, Meng Y, Liu L, Lv Y, Wei F, Yu W, Wang L, Zhang X, Ren X and Sun Q. Rational pemetrexed combined with CIK therapy plus anti-PD-1 mAbs administration sequence will effectively promote the efficacy of CIK therapy in non-small cell lung cancer. Cancer Gene Ther 2023; 30: 277-287.
[23] Wang Z, You P, Yang Z, Xiao H, Tang X, Pan Y, Li X and Gao F. PD-1/PD-L1 immune checkpoint

inhibitors in the treatment of unresectable locally advanced or metastatic triple negative breast cancer: a meta-analysis on their efficacy and safety. BMC Cancer 2024; 24: 1339.
[24] Yang L, Kartsonaki C, Simon J, Yao P, Guo Y, Lv J, Walters RG, Chen Y, Fry H, Avery D, Yu C, Jin J, Mentzer AJ, Allen N, Butt J, Hill M, Li L, Millwood IY, Waterboer T and Chen Z. Prospective evaluation of the relevance of Epstein-Barr virus antibodies for early detection of nasopharyngeal carcinoma in Chinese adults. Int J Epidemiol 2024; 53: dyae098.
[25] Liu X, Shen H, Zhang L, Huang W, Zhang S and Zhang B. Immunotherapy for recurrent or metastatic nasopharyngeal carcinoma. NPJ Precis Oncol 2024; 8: 101.
[26] Niam M, Linn YC, Fook Chong S, Lim TJ, Chu S, Choong A, Yong HX, Suck G, Chan M and Koh M. Clinical scale expansion of cytokine-induced killer cells is feasible from healthy donors and patients with acute and chronic myeloid leukemia at various stages of therapy. Exp Hematol 2011; 39: 897-903, e1.
[27] Fischer AM, Katayama CD, Pagès G, Pouysségur J and Hedrick SM. The role of erk1 and erk2 in multiple stages of T cell development. Immunity 2005; 23: 431-443.
[28] Yu X, Li W, Liu H, Wang X, Coarfa C, Cheng C, Yu X, Zeng Z, Cao Y, Young KH and Li Y. PD-L1 translocation to the plasma membrane enables tumor immune evasion through MIB2 ubiquitination. J Clin Invest 2023; 133: e160456.
[29] Liu Y, Liang X, Dong W, Fang Y, Lv J, Zhang T, Fiskesund R, Xie J, Liu J, Yin X, Jin X, Chen D, Tang K, Ma J, Zhang H, Yu J, Yan J, Liang H, Mo S, Cheng F, Zhou Y, Zhang H, Wang J, Li J, Chen Y, Cui B, Hu ZW, Cao X, Xiao-Feng Qin F and Huang B. Tumor-repopulating cells induce PD-1 expression in $CD8^+$ T cells by transferring kynurenine and AhR activation. Cancer Cell 2018; 33: 480-494, e7.
[30] Li W and Wang W. Unraveling the genetic associations between PD-1/PD-L1 and 13 circulating biomarkers linked to physiological and pathological processes. Clin Transl Oncol 2024; 26: 1157-1169.
[31] Rohit S, Patel M, Jagtap Y, Shah U, Patel A, Patel S and Solanki N. Structural Insights of PD-1/PD-L1 axis: an in silico approach. Curr Protein Pept Sci 2024; 25: 638-650.
[32] Pal R, Krishnamoorthy M, Matsui A, Kang H, Morita S, Taniguchi H, Kobayashi T, Morita A, Choi HS, Duda DG and Kumar ATN. Fluorescence lifetime imaging enables in vivo quantification of PD-L1 expression and intertumoral heterogeneity. Cancer Res 2025; 85: 618-632.
[33] Li Y, Li B, Wang Q, Zhang X, Zhang Q, Zhou X, Shi R, Wu Y, Zhai W, Chen Z, Zhou X and Zhao W. Dual targeting of TIGIT and PD-1 with a novel small molecule for cancer immunotherapy. Biochem Pharmacol 2024; 223: 116162.
[34] Yoon J, Fagan E, Jeong M and Park JH. In situ tumor-infiltrating lymphocyte therapy by local delivery of an mRNA encoding membrane-anchored anti-CD3 single-chain variable fragment. ACS Nano 2024; 18: 32401-32420.
[35] Shi S, Tao L, Song H, Chen L and Huang G. Synergistic antitumor effect of combining metronomic chemotherapy with adoptive cell immunotherapy in nude mice. APMIS 2014; 122: 380-391.
[36] Li Y, Sharma A and Schmidt-Wolf IGH. Evolving insights into the improvement of adoptive T-cell immunotherapy through PD-1/PD-L1 blockade in the clinical spectrum of lung cancer. Mol Cancer 2024; 23: 80.
[37] Patel RS, Romero R, Watson EV, Liang AC, Burger M, Westcott PMK, Mercer KL, Bronson RT, Wooten EC, Bhutkar A, Jacks T and Elledge SJ. A GATA4-regulated secretory program suppresses tumors through recruitment of cytotoxic CD8 T cells. Nat Commun 2022; 13: 256.
[38] Wang W, Li R, Meng M, Wei C, Xie Y, Zhang Y, Jiang L, Dong R, Wang C, Zhong Y, Yang F, Tang W, Jin X, Liu B and Hou Z. MicroRNA profiling of $CD3^+$ $CD56^+$ cytokine-induced killer cells. Sci Rep 2015; 5: 9571.
[39] Xiang Y, Wan F, Ren Y, Yang D, Xiang K, Zhu B, Ruan X, Li S, Zhang L, Liu X, Si Y and Liu Y. Polyphyllin VII induces autophagy-dependent ferroptosis in human gastric cancer through targeting T-lymphokine-activated killer cell-originated protein kinase. Phytother Res 2023; 37: 5803-5820.